

**Title:**

**Contribution of *rsaC*, a small non-coding RNA, towards the pathogenicity of *Staphylococcus aureus* in a mouse systemic infection model**

Suresh Panthee<sup>1,#</sup>, Hiroshi Hamamoto<sup>2,3,#</sup>, Atmika Paudel<sup>4</sup>, Suguru Ohgi<sup>5,6</sup>, Kazuhisa Sekimizu<sup>1,7,\*</sup>

<sup>1</sup> Drug Discoveries by Silkworm Models, Faculty of Pharma-Science, Teikyo University, Tokyo, Japan.

<sup>2</sup> Teikyo University Institute of Medical Mycology, Tokyo, Japan.

<sup>3</sup> Division of Sport and Health Science, Graduate School of Medical Care and Technology, Teikyo University, Tokyo, Japan.

<sup>4</sup> International Institute for Zoonosis Control, Hokkaido University, Sapporo, Japan.

<sup>5</sup> Laboratory of Microbiology, Graduate School of Pharmaceutical Sciences, The University of Tokyo, 7-3-1 Hongo, Bunkyo-ku, Tokyo 111-0033, Japan

<sup>7</sup> Genome Pharmaceuticals Institute, Ltd, Tokyo, Japan.

<sup>6</sup> Current address

Kyowa Kirin Co., Ltd., 1-9-2 Otemachi, Chiyoda-ku, Tokyo 100-0004, Japan

\* correspondence: [sekimizu@main.teikyo-u.ac.jp](mailto:sekimizu@main.teikyo-u.ac.jp)

# These authors contributed equally

**Running title:**

sRNA *rsaC* is required for full virulence of *S. aureus*

**Keywords:**

*Staphylococcus aureus*, Transcriptome analysis, virulence, sRNA, *in vivo*, pathogenicity

## 27 **Abstract**

28 Understanding how a pathogen responds to the host stimuli and succeeds in causing disease is  
 29 crucial for developing a novel treatment approach against the pathogen. Transcriptomic analysis  
 30 facilitated by RNA-Seq technologies is used to examine bacterial responses at the global level.  
 31 However, the ability to understand pathogen behavior inside the host tissues is hindered by much  
 32 lower pathogen biomass than host tissue. Recently, we succeeded in establishing a method to enrich  
 33 *Staphylococcus aureus* cells from infected organs. In this research, we analyzed the small non-  
 34 coding RNA (sRNA) transcriptome of *S. aureus* inside the host and found that *rsaC* was among the  
 35 highly expressed sRNAs. Furthermore, by gene disruption and complementation, we demonstrated  
 36 that *rsaC* was required for full pathogenicity of *S. aureus* in a murine model. Besides, we found that  
 37  $\Delta$ *rsaC* showed a difference in gene expression depending on the oxygen and host stress. The  
 38 findings of this study suggest *rsaC* acts as a novel virulence factor in *S. aureus* and might facilitate  
 39 the adaptation of *staphylococci* within the host.

## 41 **Importance**

42 Drug-resistant *Staphylococcus aureus* is among the pathogen for which new treatment options are  
 43 urgently needed. However, limited understanding of *S. aureus* pathogenesis in the host has hindered  
 44 unearthing potential strategies to treat the infections. Here, based on the *in vivo* transcriptomic  
 45 analysis, we present the identification of a small non-coding RNA (sRNA) *rsaC* as a novel  
 46 virulence factor of *S. aureus*. Furthermore, we performed transcriptomic analysis of the *rsaC*  
 47 disrupted mutant and identified different pathways, possibly controlled by *rsaC*, during aerobic,  
 48 anaerobic, and *in vivo* conditions. These findings contribute to reveal the role of sRNA *rsaC* and  
 49 broadens our understanding of the adaptation of *S. aureus* to host environments.

50

## Text

The growth and behavior of a pathogenic microorganism differ between the host environment and in the *in vitro* culture. Understanding how a pathogen responds to the host stimuli and succeeds in causing disease is crucial for developing novel drugs against the pathogen. Comprehensive transcriptomic analysis facilitated by RNA-Seq technologies using next-generation sequencers has been widely used to understand pathogen response at the global level (1, 2). Several studies have used *in vitro* host-like or *in vivo* host environments to understand the infection process and alterations in the pathogen and the host (3, 4). Such studies aimed to elucidate the functional role of protein-coding genes, while the small non-coding RNAs (sRNAs) remain largely unattended. Studies that performed the comparative analysis of pathogen response in the host to the *in vitro* growth allowed us to evaluate how a pathogen behaves during infection situations and how the host responds to pathogen invasion (4-7). The current understanding of bacterial pathogenesis allowed us to identify key virulence determinants that could potentially be exploited as a drug target for antivirulence drugs. Whereas it can be expected that pathogens lacking these virulence factors are easy to be killed or cleared from the host, their behavior in the host has not been analyzed at the global level. Furthermore, a detailed evaluation of pathogenesis requires an understanding of pathogen behavior during actual infection conditions.

sRNAs have been identified in living organisms, including the bacterial kingdom. Although they do not encode functional proteins, they can accomplish a wide range of biological functions, including regulation of gene expression at the levels of transcription, RNA processing, mRNA stability, and translation (8). In bacteria, sRNAs have the potential to regulate the gene expression pattern of the bacteria by interacting with protein or mRNAs by cis- or trans-acting mechanisms (8), thus affecting multiple cellular processes such as pathogenesis and bacterial physiology in response to environmental cues, facilitating survival under unfavorable environments. In *Staphylococcus aureus*, a pathogen of global concern, several sRNAs have been identified (9-11), while the functional characterization of this class of RNAs has long been forsaken. One of the functionally characterized and extensively studied Staphylococcal sRNA, RNAIII, regulates the expression of several virulence factors both positively and negatively (12-14). *rsaC*, a part of polycistronic operon *mntABC*, is another staphylococcal sRNA known to be expressed in infected host (15) and modulate oxidative stress during manganese starvation (16). Whereas these studies provided a hint towards its role in *S. aureus* virulence, a cell-based study showed that the  $\Delta$ *rsaC* strain was more persistent in macrophages and resistant to opsonophagocytosis than the wild-type strain (16) indicating its obscure role in pathogenesis.

We recently successfully enriched pathogen RNA from an infected animal and performed an *in vivo* RNA-Seq analysis of *Streptococcus pyogenes* (5) and *S. aureus* (6) using a two-step cell crush method. In this manuscript, we performed the comprehensive analysis of *S. aureus* sRNAs expressed within the host. Using RNA-Seq analysis of the *rsaC* disrupted mutant, we showed a clear difference between the gene expression patterns during *in vivo* and *in vitro* (aerobic and anaerobic) growth conditions. Furthermore, we found that the transcription of fermentation and oxidoreductase-related genes, virulence and toxin-related genes, and host evasion-related genes were affected during aerobic, anaerobic, and *in vivo* growth, respectively. Our results highlight the importance of *in vivo* transcriptomic analyses of two strains with the same genetic background to allow a direct comparison, revealing changes in different environments.

## Materials and Methods

### Ethics statement

All mouse experiments were performed at the University of Tokyo and Teikyo University, following the animal care and use regulations approved by the Animal Use Committee (approval numbers: P27-4 and 16-014 at respective institutes).

### Bacterial strains and primers used in the study

Bacterial strains and primers used in this study are listed in **Table 1**. *S. aureus* and *Escherichia coli* were routinely grown in LB or TSB medium, respectively, at 37°C with shaking. The media were supplemented with antibiotics, as required.

**Table 1: Bacterial strains, plasmids, and primers used in the study**

Bacteria	Relevant characteristics	Source
<i>S. aureus</i> Newman		(17)
<i>S. aureus</i> RN4220		(18)
<i>E. coli</i> HST08		Takara
<b>Plasmids and Phage</b>		
pND50-PfbaA	pND50 consisting constitutive <i>fbaA</i> promoter	(19, 20)
pSF151		(21)
pKOR3a		(22)
Phage 80α		(23)
<b>Primers</b>	<b>Sequence (5'-3')</b>	
Disruption of <i>rsaC</i>		
rsaC_U_F	GCCCTTCAGTTTTTCATCA	
rsaC_U_R	GTTCGCTAGATAGGGGTCCCCACCAAAGCGAAGTTTA	
rsaC_D_F	ATCACCTCAAATGGTTCGCTTTGTTATGTTGATGTGTGGC	
rsaC_D_R	TAAACAAGATCCACACGCA	
KmF	AGCGAACCATTTGAGGTGAT	

KmR	GGGACCCCTATCTAGCGAAC
<i>rsaC</i> complementation	
rsaC_bam_F	CGCGGATCCGCACGATATGGTGGTATTAG
rsaC_sal_R	ACGCGTCTGACTGAAAACTGAAGGGCTT
RT-PCR	
16s_rRNA_F	CAACGCGAAGAACCTTACCAA
16s_rRNA_R	GCGGGACTTAACCCAACATCT
rsaC_RT_F	AGGGAATGGCGTTGTATAAATTG
rsaC_RT_R	TCGTTCCCTTCATCTCTTTTAACC

## Real-time RT-PCR

According to the manufacturer's recommendations, one microgram of RNA was used to prepare cDNA using a High-Capacity RNA-to-cDNA<sup>TM</sup> Kit (Applied Biosystems; Foster City, CA, USA). From this, 15 ng of the cDNA was used as a template for RT-PCR using Fast SYBR Green Master Mix (Thermo Fisher Scientific) on a 7500 Fast (Applied Biosystems) machine with 40 cycles of denaturing at 95 °C followed by annealing/extension at 60 °C.

## Construction of $\Delta$ *rsaC* strain and complementation

*rsaC* was disrupted using a double cross-over recombination method as previously described (24). Briefly, the genome regions up-and down-stream of *rsaC* were amplified by PCR using the listed primers. Then, overlap extension-PCR was performed using these two DNA fragments together with the *aph* gene amplified from the pSF151 vector using primers KmF and KmR. The PCR product was cloned into the pKOR3a vector (24) and introduced into the RN4220 strain (18) by electroporation. Integration of the mutant cassette in the genome was confirmed by PCR and further transformed into *S. aureus* Newman (17) by phage transduction using phage 80 $\alpha$  as previously described (23, 25).

To prepare the overexpression strain, the *rsaC* coding region was amplified by the primer pair rsaC\_bam\_F and rsaC\_sal\_R (**Table 1**) and ligated to BamHI-SalI digested pND50-PfbaA (19, 20). The resulting plasmid, pND50-PfbaA-*rsaC*, was then transformed into *S. aureus* RN4220 by electroporation and then to *S. aureus* Newman wild and  $\Delta$ *rsaC* strains by phage transduction.

## Proteolytic and hemolytic assays

Bacteria were grown overnight in TSB medium, supplemented with antibiotics, as required, at 37°C with shaking. From this, 2  $\mu$ l aliquots were spotted on TSB containing 3.3% skim milk or sheep blood agar plates (E-MR93; Eiken Chemical, Tokyo, Japan) to determine proteolysis and hemolysis, respectively. The plates were incubated at 37°C overnight. Sealed container with Anaero Pack (Mitsubishi Gas Chemical, Tokyo, Japan) were used to determine phenotypes under anaerobic

conditions. The proteolytic and hemolytic activities were determined by the appearance of a clear zone surrounding the bacterial growth.

## Mouse survival assay

*S. aureus* Newman wild-type and  $\Delta$ *rsaC* strains were grown overnight on TSB medium supplemented with antibiotics, as required, on a rotary shaker maintained at 37 °C to obtain full growth. The full growth was diluted 100-fold with TSB and cultured overnight on the same shaker, and then the cells were centrifuged and resuspended in phosphate-buffered saline (PBS, pH 7.2) to have an optical density (OD<sub>600</sub>) of 0.7. An aliquot (200 µl) of the prepared cell suspension was then injected intravenously into C57BL/6J mouse, and mouse survival was observed. Survival analysis was performed using GraphPad Prism ver 8.0 (GraphPad Software), and statistical analysis was performed using the Log-rank (Mantel-Cox) test.

## *S. aureus* infection, organ isolation and RNA isolation

*Staphylococci* were grown overnight on TSB medium at 37°C with shaking. The full growth was diluted 100-fold with 5 ml TSB and regrown for 16h under the same conditions. The cells were centrifuged and suspended in PBS (pH 7.2). The cells (OD<sub>600</sub> = 0.7) were injected into C57BL/6J mice via the tail vein. On day 1, mice were killed to harvest organs. Organs were immediately placed either in ice to calculate viable cell numbers in each organ or liquid nitrogen and maintained at -80 °C for RNA extraction. Each experiment was conducted with three animals, and data are represented as an average. Mouse organs were homogenized, and total RNA was extracted, as explained previously (6). RNA extraction from *in vitro* culture was performed as explained (19). For anaerobic RNA-Seq, staphylococci were first grown aerobically to reach OD<sub>600</sub> of 1.0 and then transferred to anaerobic growth for 30 minutes.

## Library preparation and RNA-sequencing

Total RNA was subjected to rRNA depletion using a MICROBExpress™ Kit (Thermo Fisher Scientific, Waltham, MA) and used for library preparation for RNA-Seq using an Ion Total RNA-Seq Kit v2 following the manufacturer's instructions. After confirming the size distribution and yield of the amplified library using a bioanalyzer, the libraries were enriched in an Ion PI Chip v2 using the Ion Chef (Thermo Fisher Scientific) and sequenced using Ion Proton System (Thermo Fisher Scientific). These data have been deposited in the NCBI Sequence Read Archive under accession number #####.

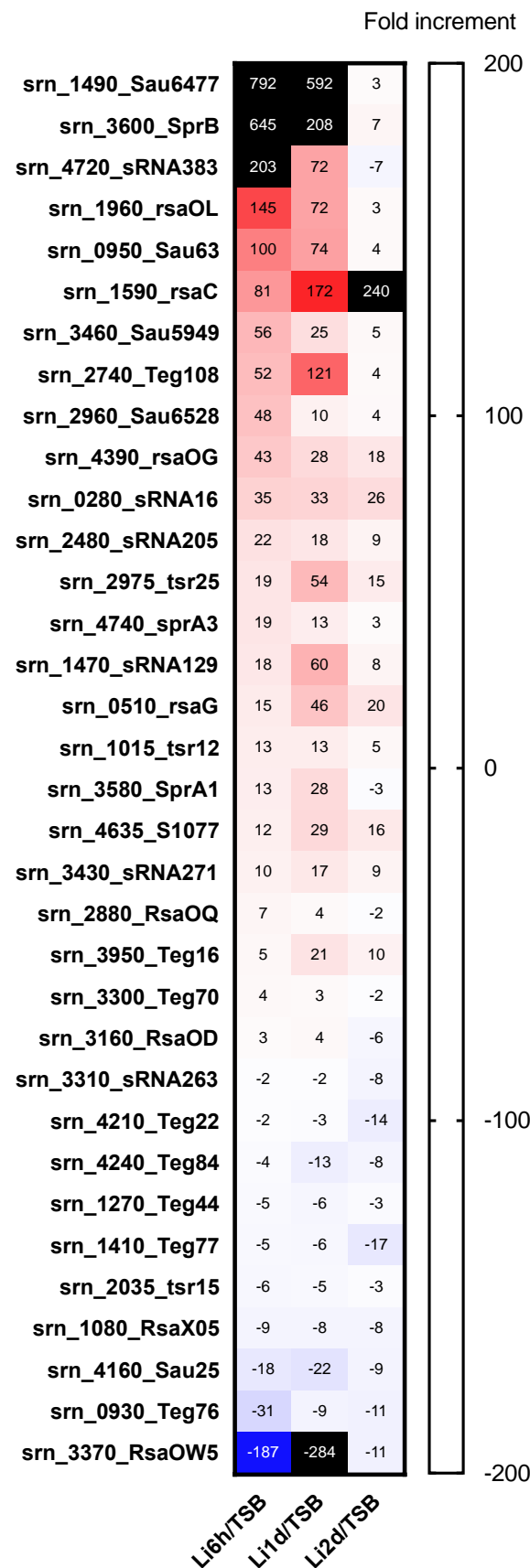
## Differential gene expression analysis

All data were analyzed using CLC Genomics Workbench software, version 21.0.4 (CLC Bio, Aarhus, Denmark). Reads were aligned to the Newman genome annotated with ncRNA genes allowing a minimum length fraction of 0.95 and a minimum similarity fraction of 0.95. Differential gene expression analysis was performed using the default setting. Genes with a false discovery rate (FDR)  $p < 0.05$  were classified as having significantly different expressions.

## Results

### Comprehensive analysis of sRNAs expression in the host environment

To quantitatively analyze the expression of *S. aureus* sRNAs within the host, we first annotated the sRNAs present in the Newman strain based on the report of Sassai *et al.* (11). Next, we performed an RNA-Seq analysis based on the reads obtained from our two-step cell crush method (6). A comparative expression analysis of RNA isolated from host liver at 6- hr, 1- day and 2- day post-infection to the RNA isolated from *in-vitro* culture was performed. We found that among 559 sRNAs present, 34 sRNAs were differentially expressed at all the three-time points compared to *in vitro* (**Figure 1**). Upregulation or downregulation of these sRNAs at all three time points suggested these sRNAs' possible role to respond to host circumstances.



189

190 **Figure 1. Expression of staphylococcal sRNAs in the host environment.** Differential expression  
 191 of Newman sRNAs in mouse liver compared to TSB medium culture condition. sRNAs with  
 192 common differential expression and FDR  $p < 0.05$  on all the three-time points are shown.

193

## 194 Identification of RsaC as a virulence factor

195 Given that many sRNAs were differentially expressed under the host circumstances, we  
 196 were interested in whether these sRNAs can modulate *S. aureus* pathogenesis. Among sRNAs, we  
 197 focused on *rsaC*, as it falls among one of the studied staphylococcal sRNAs. Previously, *rsaC* was  
 198 shown to have an increased expression in the infected host (15) and modulate oxidative stress  
 199 during manganese starvation (16). However, its role in the regulation of pathogenesis has remained  
 200 elusive. First, we confirmed the expression of *rsaC* in mouse organs using a real-time reverse  
 201 transcription-polymerase chain reaction (RT-PCR). A higher expression of *rsaC* was observed in  
 202 both the kidney and liver, as compared to TSB medium culture condition (**Figure 2A**). The gene  
 203 organization of *rsaC* in the Newman genome (**Figure 2B**) showed that *rsaC* did not overlap with  
 204 other genes, allowing us to construct a single gene disruption mutant. We constructed the *rsaC*  
 205 disrupted mutant and examined its role in pathogenicity using a mouse infection model. We found  
 206 that  $\Delta$ *rsaC* had reduced ability to colonize in mouse heart 24h post-infection whereas the ability to  
 207 colonize in kidney, liver, lungs and spleen were indistinguishable from that of the wild-type  
 208 (**Figure 2C**). To further confirm the role of *rsaC* in virulence, we checked the survival of wild-type  
 209 or  $\Delta$ *rsaC*- infected mice. The results indicated that the  $\Delta$ *rsaC* strain had reduced virulence (**Figure**  
 210 **2D**), evident by prolonged survival of the  $\Delta$ *rsaC* infected mice. To eliminate the possibilities of  
 211 polar effects associated with this disruption on pathogenicity, we complemented the wild-type and  
 212 the  $\Delta$ *rsaC* strains by reintroducing *rsaC* under the control of a constitutive promoter- *PfbaA*.  
 213 Restored pathogenicity of the complemented strain unequivocally explained the involvement of  
 214 *rsaC* in pathogenicity and established it as a virulence factor of *S. aureus*.

215

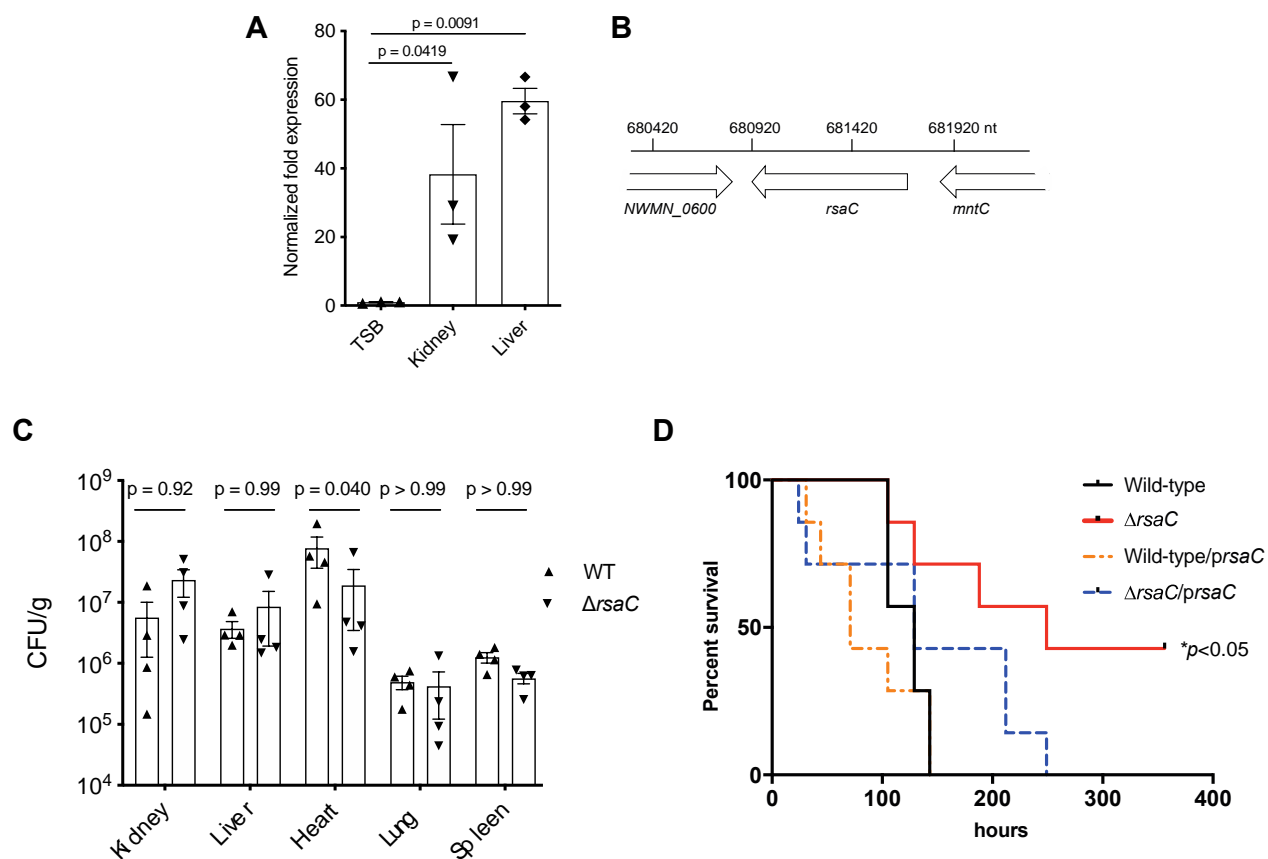
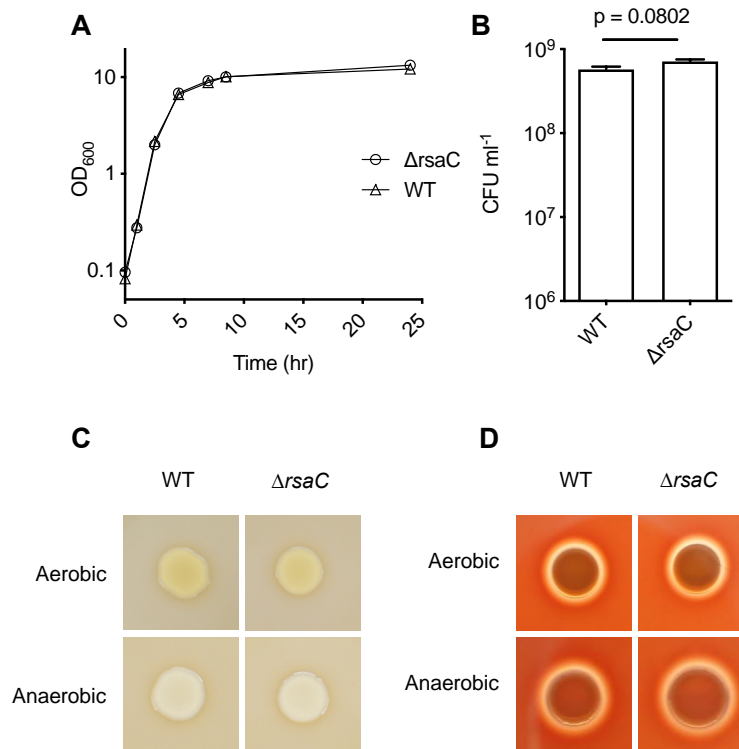


**Figure 2. In vivo expression and involvement of RsaC in the pathogenesis of *S. aureus*.** (A) Upregulation of *rsaC* in host organs compared with that in TSB medium was confirmed by RT-PCR. The data were standardized by the abundance of 16s rRNA in each sample, and statistical analysis was performed using ANOVA. (B) Position of the *rsaC* in *S. aureus* Newman chromosome. (C) The number of *S. aureus* cells in each organ after infection with ( $7.6 \times 10^7$  CFU and  $7.5 \times 10^7$  CFU) *S. aureus* Newman and  $\Delta$ rsaC strains, respectively. Statistical analysis was performed using 2way ANOVA with Sidak's multiple comparisons in GraphPad Prism 8.4.3. (D) Survival of mice after the infection with a deletion mutant of the *rsaC* gene. Wild-type,  $\Delta$ rsaC, wild-type/prsaC, or  $\Delta$ rsaC/prsaC were injected intravenously at a dose of  $5.0 \times 10^7$ ,  $5.9 \times 10^7$ ,  $4.8 \times 10^7$  and  $5.0 \times 10^7$  CFU, respectively. Asterisk indicates a significant difference compared with the survival curve following wild-type injection ( $p < 0.05$ ) by the Log-rank (Mantel-Cox) test. The experiment was performed two times, and essentially the same results were obtained.

Next, we performed the phenotypic evaluation of the  $\Delta$ rsaC mutant *in vitro*. We found that the growth of  $\Delta$ rsaC strain was indistinguishable from that of the wild-type during both aerobic (**Figure 3A**) and anaerobic (**Figure 3B**) growth. In addition,  $\Delta$ rsaC had unaltered proteolytic and hemolytic abilities compared to that of the wild-type during both aerobic and anaerobic culture conditions (**Figure 3C, D**). These results suggested no difference between the wild-type and mutant

235 in terms of virulence-related *in vitro* phenotypes and necessitated an *in vivo* infection system to  
 236 investigate the role of *rsaC* in pathogenesis.  
 237



238  
 239 **Figure 3. *In vitro* phenotypic analysis of *rsaC* disruption.**

240 (A) Growth curve of  $\Delta rsaC$  and wild-type strains during aerobic culture. (B) Colony Forming  
 241 Units (CFUs) of  $\Delta rsaC$  and wild-type strains after growing anaerobically. Statistical analysis was  
 242 performed using an unpaired t-test. (C) Proteolytic- and (D) hemolytic- ability of  $\Delta rsaC$  and wild-  
 243 type strains during aerobic and anaerobic conditions.

244

## 245 **Role of *rsaC* in *S. aureus* transcriptome**

246 Given that *in vitro* phenotypic analysis could not elucidate the possible link between the  
 247 *rsaC* disruption and pathogenicity, we aimed to examine the transcriptome at the global level. We  
 248 compared the gene expression pattern by performing an RNA-Seq analysis of the  $\Delta rsaC$  and the  
 249 wild-type strains under multiple growth conditions- aerobic, anaerobic, and *in vivo* (**Figure 4A**).  
 250 Since we found higher colonization of *S. aureus* in the heart compared to other organs, and the  
 251  $\Delta rsaC$  strain tended to colonize less in the heart compared to the wild-type (**Figure 2D**), we  
 252 selected heart for *in vivo* RNA-Seq. The gene expression patterns of the  $\Delta rsaC$  strain was compared  
 253 to that of the wild-type strain in different growth conditions revealing the differential expression of  
 254 diverse genes in the three tested conditions. Whereas 29, 254, and 47 genes were differentially  
 255 expressed on RNA obtained from aerobic-growth, anaerobic-growth, and mouse heart, respectively,  
 256 no commonly affected genes were observed (**Figure 4B**). This indicated a difference in the gene

expression pattern depending on growth conditions. Fermentation-related genes, most of which are also associated with the oxidoreductase activity, were downregulated in the  $\Delta rsaC$  mutant when grown under aerobic conditions (**Figure 4C, Table 2**). Based on this, we speculated that *rsaC* directs *S. aureus* towards fermentative respiration by acting as a regulator of fermentation. Under anaerobic conditions, we found the downregulation of many transporters, virulence-related genes in  $\Delta rsaC$  mutant (**Figure 4D, Table 2**). The *in vivo* RNA-Seq analysis, performed in mouse heart at 24 -hr post-infection, showed that compared to wild-type strains, genes related to metal ion (copper and potassium) acquisition and virulence (related to tissue invasion, evasion of host defense, and inhibition of neutrophil activation) were significantly downregulated in the  $\Delta rsaC$  strain (**Figure 4E, Table 2**), which suggested the possible role of host stress towards pathogen response. Taken together, these results indicate the diverse functions of *rsaC* during aerobic, anaerobic, and *in vivo* growth.

We further categorized the differentially expressed genes depending on their up-and down-regulated status and performed a PANTHER overrepresentation test. We found that genes related to oxidoreductase activity were overrepresented among the genes downregulated in aerobic conditions (**Table 3**). Conversely, among the genes upregulated during the anaerobic condition, the genes related to protein folding and translation were overrepresented, and the genes involved in transmembrane transport were underrepresented (**Table 3**). A previous study also found that these genes are upregulated in anaerobic conditions (26).

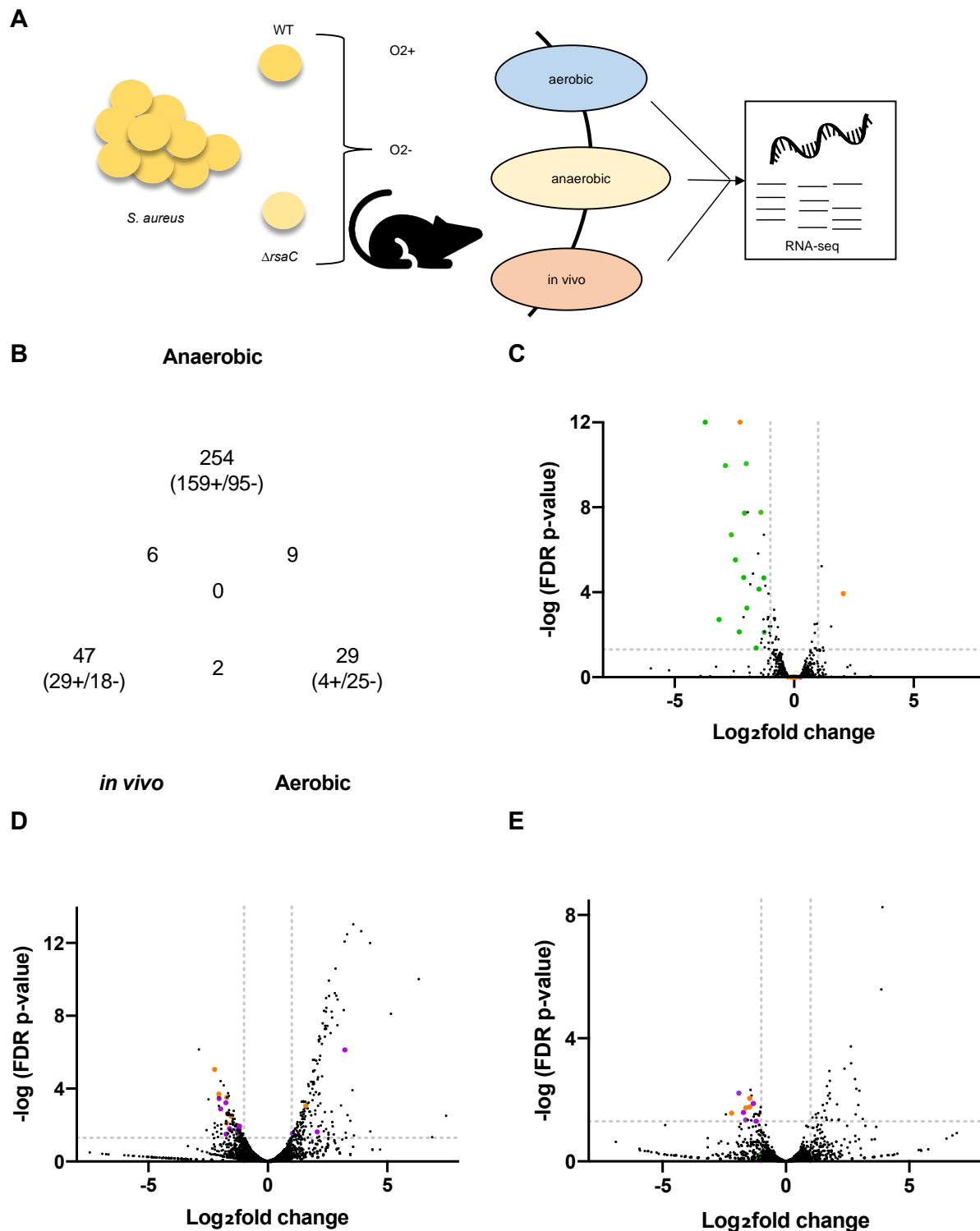


**Figure 4. Global transcriptomic analysis of *rsaC* disruption in *S. aureus*.** (A) Experimental model to perform transcriptomic analysis. (B) Venn diagram showing the genes with common differential expression between *in vitro* (aerobic and anaerobic) and *in vivo* (heart). A volcano plot showing the genes differentially expressed in the  $\Delta$ *rsaC* strain, compared to wild-type during (C) aerobic, (D) anaerobic, and (E) *in vivo* (heart) growth. Genes involved in fermentation, virulence, and metal-ion acquisition are colored green, orange, and purple, respectively. Data points outside the dotted lines along the y-axis represent fold changes of  $\geq 2.0$  and that along the x-axis represent

286 FDR  $p \leq 0.05$ . The complete list of differentially expressed genes is presented in the supplementary  
287 dataset.

288

289 **Table 2: Fermentation, virulence, and metal ion acquisition-related genes differentially**  
290 **expressed (FDR  $p < 0.05$  in the  $\Delta$ rsaC strain compared to wild-type) during aerobic,**  
291 **anaerobic, and *in vivo* growth.**

Gene name	Gene product	$\Delta$ rsaC vs. WT during					
		aerobic		anaerobic		<i>in vivo</i>	
		Fold	FDR p	Fold	FDR p	Fold	FDR p
Category: Fermentation							
pflB	formate acetyltransferase	-13.18	0.00	1.50	0.44	-1.23	0.90
lctE	L-lactate dehydrogenase	-8.84	0.00	2.13	0.04	-1.60	0.76
pflA	pyruvate formate-lyase-activating enzyme	-7.33	0.00	2.40	0.03	-1.22	0.90
nirR	cobalamin biosynthesis protein CbiX	-6.18	0.00	1.51	0.43	-1.28	0.88
lctP	L-lactate permease	-5.48	0.00	-1.85	0.13	-1.12	0.95
adh1	zinc-dependent alcohol dehydrogenase	-4.32	0.00	2.31	0.02	-1.68	0.69
ilvA	serine/threonine dehydratase	-4.22	0.00	-1.99	0.10	-1.72	0.56
nasD, nirB	nitrite reductase large subunit	-4.02	0.00	1.13	0.87	-1.24	0.88
ald	alanine dehydrogenase	-3.95	0.00	-1.24	0.72	-1.83	0.47
nasE, nirD	nitrite reductase (NAD(P)H) small subunit	-3.00	0.04	-1.51	0.40	-1.38	0.85
adhE	bifunctional acetaldehyde-CoA/alcohol dehydrogenase	-2.77	0.00	-1.27	0.70	-1.85	0.62
ddh	lactate dehydrogenase	-2.63	0.00	1.37	0.49	1.05	0.98
ndhF	NADH dehydrogenase subunit 5	-2.40	0.00	-1.08	0.93	1.19	0.93
NWMN_RS13240	formate/nitrite transporter	-1.03	1.00	-2.39	0.03	-1.34	0.76
NWMN_RS01365	formate/nitrite transporter	-4.92	0.01	-1.44	0.43	1.14	0.91
narK, narT	MFS transporter	-2.37	0.01	1.11	0.90	-2.02	0.63
Category: Virulence							
ccpA	catabolite control protein A	1.05	1.00	-4.69	0.00	1.02	0.99
agrB	accessory gene regulator AgrB	-1.06	1.00	-4.14	0.00	-1.97	0.53
hlgB	gamma-hemolysin component B	-1.08	1.00	-3.30	0.01	-1.73	0.84
lukF	Leukocidin/Hemolysin toxin family protein	-1.02	1.00	-3.29	0.00	-1.07	0.98
mgrA	MarR family transcriptional regulator	1.04	1.00	-3.20	0.00	-1.27	0.88
lukS	Aerolysin/Leukocidin family protein	1.01	1.00	-2.91	0.00	-1.09	0.98
agrC	ATP-binding protein	-1.04	1.00	-2.40	0.02	-1.77	0.76
sak	staphylokinase			-1.93	0.73	-4.59	0.03
sspB	staphopain A	1.06	1.00	-1.15	0.91	-3.09	0.02
eta	permease	-1.20	1.00	-1.32	0.64	-2.75	0.02
nsaS		-1.02	1.00	-1.02	0.98	-2.76	0.01
spa	peptidoglycan-binding protein LysM	-4.80	0.00	3.00	0.00	1.64	0.45
Category: Metal-ion acquisition							
opuCD	amino acid ABC transporter permease	1.20	1.00	-3.38	0.00	1.26	0.82
NWMN_RS03330	iron ABC transporter permease	-1.06	1.00	-3.36	0.03	-1.08	0.94
NWMN_RS09470	calcium-binding protein	-1.81	0.08	-3.04	0.02	-1.69	0.51

NWMN_RS12570	molybdenum cofactor biosynthesis protein	1.13	1.00	<b>-2.29</b>	0.02	1.08	0.96
copZ	copper chaperone CopZ	1.06	1.00	1.76	0.45	<b>-3.30</b>	0.03
narJ	nitrate reductase molybdenum cofactor assembly chaperone	1.11	1.00	<b>-4.11</b>	0.00	-1.64	0.84
NWMN_RS03330	iron ABC transporter permease	-1.06	1.00	<b>-3.36</b>	0.03	-1.08	0.94
NWMN_RS09470	calcium-binding protein	-1.81	0.08	<b>-3.04</b>	0.02	-1.69	0.51
mnhC, mnhC1	Na(+)/H(+) antiporter subunit C	-1.03	1.00	<b>-3.93</b>	0.00	1.10	0.93
NWMN_RS08175	MBL fold metallo-hydrolase	1.09	1.00	<b>2.04</b>	0.03	-1.19	0.88
putP	sodium:proline symporter	1.02	1.00	<b>-2.45</b>	0.02	1.10	0.93
cobI	magnesium transporter CorA	1.14	1.00	<b>-2.39</b>	0.03	-1.12	0.91
sirA	iron ABC transporter substrate-binding protein	-1.17	1.00	<b>4.18</b>	0.02	-1.06	0.97
sitC, mntC	metal ABC transporter substrate-binding protein	1.68	0.02	<b>9.32</b>	0.00	1.76	0.63
NWMN_RS03420	sodium:proton antiporter	1.10	1.00	<b>-2.28</b>	0.01	<b>-2.49</b>	0.01
cztB	cation transporter	1.07	1.00	<b>-2.88</b>	0.00	<b>-2.30</b>	0.05
kdpB	potassium-transporting ATPase subunit B	1.26	0.86	1.09	0.95	<b>-3.09</b>	0.04
cztAf	zinc/cobalt-responsive transcriptional repressor	1.164	0.999	-1.1	0.901	<b>-3.7</b>	0.006

**Table 3: Significantly overrepresented or underrepresented groups among the genes differentially expressed in the *ΔrsaC* strain.**

Downregulated in aerobic	Fold Enrichment	FDR p
<b>GO molecular function</b>		
oxidoreductase activity	4.83	3.63E-02
Upregulated in anaerobic	Fold Enrichment	FDR p
<b>GO biological process</b>		
'de novo' protein folding	21.89	2.17E-02
protein folding	15.92	8.31E-05
chaperone-mediated protein folding	21.89	2.06E-02
translation	6.65	1.99E-12
peptide biosynthetic process	6.11	7.24E-12
peptide metabolic process	5.61	3.62E-11
organonitrogen compound metabolic process	1.85	1.51E-03
cellular amide metabolic process	4.19	5.64E-09
cellular nitrogen compound metabolic process	1.71	3.41E-02
amide biosynthetic process	5.27	4.43E-11
cellular nitrogen compound biosynthetic process	2.67	1.27E-05
organonitrogen compound biosynthetic process	2.24	5.30E-04
organic substance biosynthetic process	1.71	4.55E-02
gene expression	3.59	1.77E-07
macromolecule metabolic process	1.93	1.18E-03
cellular macromolecule biosynthetic process	3.25	7.92E-07
cellular macromolecule metabolic process	2.18	2.78E-04
macromolecule biosynthetic process	3.22	8.76E-07
cellular protein metabolic process	4.28	1.78E-10
protein metabolic process	3.66	2.32E-10
primary metabolic process	1.54	3.27E-02
transmembrane transport	0.08	7.89E-03
<b>GO molecular function</b>		
unfolded protein binding	14.59	6.33E-03
structural constituent of ribosome	11.14	2.09E-16
structural molecule activity	11.14	1.05E-16
rRNA binding	8.65	1.02E-07
RNA binding	3.91	4.99E-05
transmembrane transporter activity	0.09	3.83E-02
transporter activity	0.09	3.29E-02
<b>GO cellular component</b>		
cytosolic large ribosomal subunit	10.1	3.92E-07
cytosolic ribosome	9.85	2.30E-10
cytosol	2.25	3.31E-04
cytoplasm	1.84	1.15E-04
intracellular anatomical structure	2.13	1.79E-08
ribosome	10.94	1.70E-18

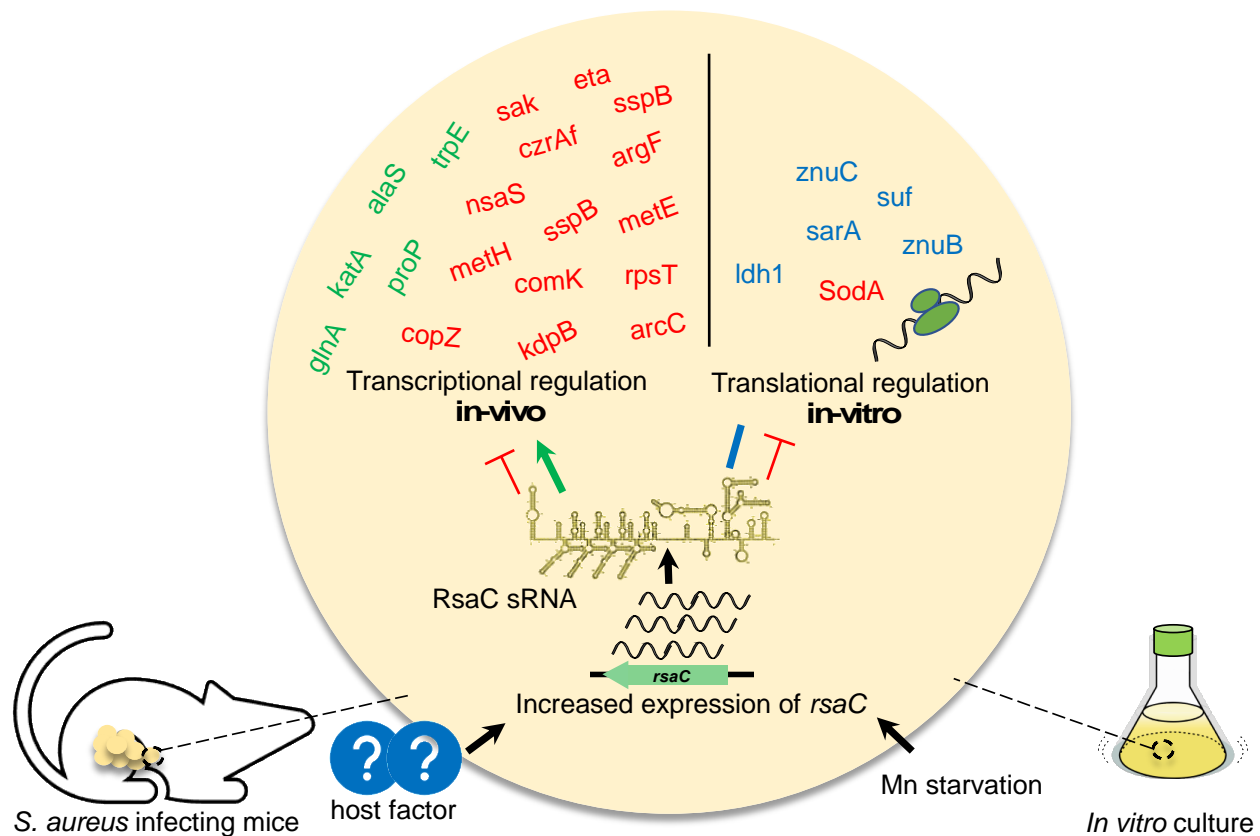
intracellular non-membrane-bounded organelle	8.75	3.74E-17
intracellular organelle	7.45	2.68E-16
organelle	7.45	2.14E-16
non-membrane-bounded organelle	8.75	2.50E-17
large ribosomal subunit	9.73	5.07E-07
ribosomal subunit	9.12	6.07E-11
ribonucleoprotein complex	8.58	1.28E-10
protein-containing complex	2.74	2.04E-04
cytosolic small ribosomal subunit	9.38	1.17E-03
small ribosomal subunit	8.34	2.11E-04
integral component of membrane	0.22	3.18E-07
intrinsic component of membrane	0.22	2.94E-07
membrane	0.2	7.28E-09
plasma membrane	0.21	4.02E-04
cell periphery	0.25	9.19E-04

## Discussion

In this manuscript, we identified a Staphylococcal sRNA *rsaC* as a virulence factor, required for full virulence of *S. aureus*. Despite some studies involving *rsaC* (15, 16), its participation in pathogenesis was obscure. Our results suggested that RsaC regulates *S. aureus* transcriptome differently, depending on oxygen availability and host stress. For instance, during aerobic conditions where cells tend to use O<sub>2</sub> as a terminal electron acceptor (27, 28), we found that RsaC was directing the cells towards anaerobic respiration. Besides, anaerobic conditions, such as those encountered *in vivo* and exaggerated by pathogen colonization and heart failure (6) might lead to the adaptation to adverse environment by regulating nutrition acquisition and virulence factor production, at least partly by the sRNA *rsaC*.

We also found that many genes involved in metal acquisition were downregulated during anaerobic and *in vivo* conditions. Lalaouna et al elucidated the role of *rsaC* in regulating oxidative stress during manganese starvation and identified an Mn-dependent superoxide dismutase *sodA* mRNA as the target of *rsaC* (16). They also found that RsaC interacts of *sodA* mRNA and affects the posttranslational events (16). In our RNA-Seq analysis, we did not find the differential expression of *sodA* in any of the three different growth conditions tested, indicating that *rsaC* does not affect *sodA* at transcriptional level. Thus, our approach of comparing less-virulent strain with its counter virulent strain under different conditions led to the findings that *rsaC* has diverse roles dependent upon the environment encountered by *S. aureus*, yet there existed some commonalities. The gene expression in aerobic condition implied that *rsaC* was involved in shifting bacterial cells from aerobic to anaerobic respiration state; that in anaerobic condition revealed that *rsaC* was involved in metal acquisition and toxin production; and that during *in vivo* condition uncovered that *rsaC* was involved in virulence through host invasion and inhibiting the activation of neutrophils. Therefore, based on previous study (16) and this study, RsaC functions as a transcriptional and

322 translational regulator of a wide variety of genes (**Figure 5**) which ultimately play a role in  
323 virulence, a detailed mechanism of which is yet to be identified.



324  
325 **Figure 5.** Role of RsaC in gene regulation *in vivo* and *in vitro*. Unknown host factors (*in vivo*) or  
326 Mn starvation (*in vitro*) trigger the expression of *rsaC*, which regulates the expression of several  
327 genes (this study) or binds to several mRNAs and regulate their translation (16). Red, green, and  
328 blue color indicate negative regulation, positive regulation, and binding with unknown effect,  
329 respectively.

330  
331 Further, we observed the upregulation of genes involved in translation, protein folding, and  
332 oxidative stress during anaerobic condition. Since clear role of these genes in virulence remains  
333 unknown, we speculate that the regulation of translation and protein folding could be a secondary  
334 effect of *rsaC* disruption. For instance, in manganese depleted environment, *rsaC* modulated SodM  
335 that can use iron as the cofactor for ROS detoxification (16). A detailed understanding of *rsaC*  
336 upregulation inside hosts and how RsaC controls gene expression at transcriptional, translational,  
337 and posttranslational levels requires further investigation. We searched for partially homologous  
338 sequences to the *rsaC* gene in whole genome sequence of the Newman strain that could be targets  
339 of transcriptional regulation by RsaC, however; were unable to find any regions. Nonetheless, this  
340 key finding of the involvement of RsaC in the virulence of *S. aureus* led to the identification of

novel virulence sRNA and opened up avenues for the development of novel antimicrobial agents to treat severe systemic infection by targeting the RsaC signaling pathway.

## Acknowledgements

This work was supported by JSPS KAKENHI Grant Numbers 19K07140JP, 15H05783, 26102714, 24689008, the Mochida Memorial Foundation for Medical and Pharmaceutical Research, and the Takeda Science Foundation to H.H., and in part by JSPS KAKENHI Grant Numbers 19K16653, 20K16253, 21H02733, and JP17F17421, TBRF, IFO fellowships to S.P. and K.S.

## Author contributions

S.P. and H.H. conceived the idea. S.P., H.H. and A.P. performed *in vivo* RNA-Seq analysis. S.P. and A.P. wrote the manuscript. S.O. prepared the gene disruptant mutants. H.H., S.P., A.P., and S.O. performed the mouse systemic infection assays. S.P. performed real time RT-PCR and *in vitro* phenotypic analysis. K.S. critically revised the article for important intellectual content and provided final approval of the article.

## Competing interests

K.S. is a consultant for Genome Pharmaceutical Institute Co., Ltd.

## References

- Colgan AM, Cameron AD, Kroger C. 2017. If it transcribes, we can sequence it: mining the complexities of host-pathogen-environment interactions using RNA-seq. *Curr Opin Microbiol* 36:37-46.
- Creedy JP, Conway T. 2015. Quantitative bacterial transcriptomics with RNA-seq. *Curr Opin Microbiol* 23:133-40.
- Ishii K, Adachi T, Yasukawa J, Suzuki Y, Hamamoto H, Sekimizu K. 2014. Induction of virulence gene expression in *Staphylococcus aureus* by pulmonary surfactant. *Infect Immun* 82:1500-1510.
- Westermann AJ, Förstner KU, Amman F, Barquist L, Chao Y, Schulte LN, Müller L, Reinhardt R, Stadler PF, Vogel J. 2016. Dual RNA-seq unveils noncoding RNA functions in host-pathogen interactions. *Nature* 529:496-501.
- Hirose Y, Yamaguchi M, Okuzaki D, Motooka D, Hamamoto H, Hanada T, Sumitomo T, Nakata M, Kawabata S. 2019. *Streptococcus pyogenes* Transcriptome Changes in the Inflammatory Environment of Necrotizing Fasciitis. *Appl Environ Microbiol* 85.
- Hamamoto H, Panthee S, Paudel A, Suguru O, Suzuki Y, Sekimizu K. 2021. Transcriptome change in *Staphylococcus aureus* in infecting mice. *Nature Portfolio* doi:10.21203/rs.3.rs-636230/v1.

- 379 7. D'Mello A, Riegler AN, Martinez E, Beno SM, Ricketts TD, Foxman EF, Orihuela CJ,  
380 Tettelin H. 2020. An in vivo atlas of host-pathogen transcriptomes during *Streptococcus*  
381 *pneumoniae* colonization and disease. *Proc Natl Acad Sci U S A* 117:33507-33518.
- 382 8. Caldelari I, Chao Y, Romby P, Vogel J. 2013. RNA-Mediated Regulation in Pathogenic  
383 Bacteria. *Cold Spring Harbor Perspectives in Medicine* 3.
- 384 9. Guillet J, Hallier M, Felden B. 2013. Emerging functions for the *Staphylococcus aureus*  
385 RNome. *PLOS Pathog* 9:e1003767.
- 386 10. Kaito C, Omae Y, Matsumoto Y, Nagata M, Yamaguchi H, Aoto T, Ito T, Hiramatsu K,  
387 Sekimizu K. 2008. A novel gene, *fudoh*, in the SCCmec region suppresses the colony  
388 spreading ability and virulence of *Staphylococcus aureus*. *PLoS One* 3:e3921.
- 389 11. Sassi M, Augagneur Y, Mauro T, Ivain L, Chabelskaya S, Hallier M, Sallou O, Felden B.  
390 2015. SRD: a *Staphylococcus* regulatory RNA database. *RNA* 21:1005-1017.
- 391 12. Boisset S, Geissmann T, Huntzinger E, Fechter P, Bendridi N, Possedko M, Chevalier C,  
392 Helfer AC, Benito Y, Jacquier A, Gaspin C, Vandenesch F, Romby P. 2007. *Staphylococcus*  
393 *aureus* RNAIII coordinately represses the synthesis of virulence factors and the transcription  
394 regulator Rot by an antisense mechanism. *Genes Dev* 21:1353-66.
- 395 13. Huntzinger E, Boisset S, Saveanu C, Benito Y, Geissmann T, Namane A, Lina G, Etienne J,  
396 Ehresmann B, Ehresmann C, Jacquier A, Vandenesch F, Romby P. 2005. *Staphylococcus*  
397 *aureus* RNAIII and the endoribonuclease III coordinately regulate *spa* gene expression.  
398 *EMBO J* 24:824-35.
- 399 14. Gupta RK, Luong TT, Lee CY. 2015. RNAIII of the *Staphylococcus aureus* agr system  
400 activates global regulator MgrA by stabilizing mRNA. *Proc Natl Acad Sci U S A*  
401 112:14036-41.
- 402 15. Szafranska AK, Oxley APA, Chaves-Moreno D, Horst SA, Roßlenbroich S, Peters G,  
403 Goldmann O, Rohde M, Sinha B, Pieper DH, Löffler B, Jauregui R, Wos-Oxley ML,  
404 Medina E. 2014. High-resolution transcriptomic analysis of the adaptive response of  
405 *Staphylococcus aureus* during acute and chronic phases of osteomyelitis. *mBio* 5.
- 406 16. Lalaouna D, Baude J, Wu Z, Tomasini A, Chicher J, Marzi S, Vandenesch F, Romby P,  
407 Caldelari I, Moreau K. 2019. RsaC sRNA modulates the oxidative stress response of  
408 *Staphylococcus aureus* during manganese starvation. *Nucleic Acids Res* 47:9871-9887.
- 409 17. Duthie ES, Lorenz LL. 1952. *Staphylococcal* coagulase; mode of action and antigenicity. *J*  
410 *Gen Microbiol* 6:95-107.
- 411 18. Peng HL, Novick RP, Kreiswirth B, Kornblum J, Schlievert P. 1988. Cloning,  
412 characterization, and sequencing of an accessory gene regulator (*agr*) in *Staphylococcus*  
413 *aureus*. *J Bacteriol* 170:4365-72.
- 414 19. Paudel A, Panthee S, Hamamoto H, Grunert T, Sekimizu K. 2021. YjbH regulates virulence  
415 genes expression and oxidative stress resistance in *Staphylococcus aureus*. *Virulence*  
416 12:470-480.
- 417 20. Paudel A, Hamamoto H, Panthee S, Matsumoto Y, Sekimizu K. 2020. Large-Scale  
418 Screening and Identification of Novel Pathogenic *Staphylococcus aureus* Genes Using a  
419 Silkworm Infection Model. *J Infect Dis* 221:1795-1804.
- 420 21. Tao L, LeBlanc DJ, Ferretti JJ. 1992. Novel streptococcal-integration shuttle vectors for  
421 gene cloning and inactivation. *Gene* 120:105-10.
- 422 22. Bae T, Schneewind O. 2006. Allelic replacement in *Staphylococcus aureus* with inducible  
423 counter-selection. *Plasmid* 55:58-63.
- 424 23. Novick RP. 1991. Genetic systems in *staphylococci*. *Methods Enzymol* 204:587-636.
- 425 24. Kaito C, Hirano T, Omae Y, Sekimizu K. 2011. Digestion of extracellular DNA is required  
426 for giant colony formation of *Staphylococcus aureus*. *Microbial Pathogenesis* 51:142-148.
- 427 25. Paudel A, Hamamoto H, Panthee S, Kaneko K, Matsunaga S, Kanai M, Suzuki Y, Sekimizu  
428 K. 2017. A novel spiro-heterocyclic compound identified by the silkworm infection model  
429 inhibits transcription in *Staphylococcus aureus*. *Front Microbiol* 8:712.

- 430 26. Fuchs S, Pané-Farré J, Kohler C, Hecker M, Engelmann S. 2007. Anaerobic Gene  
431 Expression in Staphylococcus aureus. Journal of Bacteriology 189:4275-4289.
- 432 27. Babcock GT. 1999. How oxygen is activated and reduced in respiration. Proc Natl Acad Sci  
433 U S A 96:12971-3.
- 434 28. Borisov VB, Verkhovsky MI. 2015. Oxygen as Acceptor. EcoSal Plus 6.  
435